Journal of Alloys and Compounds 577 (2013) 170–173

Contents lists available at SciVerse ScienceDirect

Journal of Alloys and Compounds

journal homepage: www.elsevier.com/locate/jalcom

White light emission, quantum cutting, and afterglow luminescence of Eu^{3+}-doped $Ba_5Gd_8Zn_4O_{21}$

Yanmin Yang *, Ziqiang Li, Zhiqiang Li, Fuyun Jiao, Xianyuan Su, Dayong Ge

Luminescence and Display Research Institute, College of Physics Science and Technology, Hebei University, Baoding 071002, China

ARTICLE INFO

Article history:
Received 23 March 2013
Received in revised form 25 April 2013
Accepted 27 April 2013
Available online 6 May 2013

Keywords:
Phosphors
White light emission
Quantum cutting
X-ray
Afterglow

ABSTRACT

$Ba_5Gd_8Zn_4O_{21}$:xEu^{3+} (x = 0.05%, 0.5%, 1%, 2%, 5%, and 10%) phosphors were prepared by a conventional high-temperature solid-state reaction. White light emission was generated by the combined $^5D_{0,1,2,3}$–$^7F_{0,1,2,3}$ transitions of Eu^{3+} in $Ba_5Gd_8Zn_4O_{21}$ under 395 nm excitation. More interestingly, when the same phosphor was excited by ultraviolet (274 nm) and X-ray, the intense red emission were achieved and it is interpreted by efficient quantum cutting between Gd^{3+} and Eu^{3+}. The cutting efficiency of $Ba_5Gd_8Zn_4O_{21}$:1%Eu^{3+} was calculated to be around 169% under X-ray excitation. Furthermore, after X-ray irradiation, the phosphors showed an intense long-lived afterglow luminescence and the luminescence can be modulated via sintering temperature.

1. Introduction

For many years, rare earth (RE) ions doped luminescence materials draw much attention due to their practical importance in many fields such as display devices, lighting sources, and detection [1–6]. Particularly, white light-emitting diodes (W-LEDs) are considered as the next generation light source due to their high brightness, long lifetime and environment friendliness. The current commercial W-LEDs were fabricated by combining a blue-emitting LED chip with a yellow-emitting phosphor (YAG: Ce^{3+}). However, this type of white LED has low color rendering index, which is not very suitable for solid-state lighting [6]. The above drawback could be dissolved by using ultraviolet LED chip exciting red, green and blue tricolor phosphors [7]. The other high energy excitation sources, such as cathode-ray tubes, field, and plasma, have also found wide promising applications in display field. However, all of these materials suffer from great energy loss. Quantum cutting (QC), in which one higher energy photon can be transformed into two or more lower ones, is considered as the most efficient way to solve the energy loss [8]. Investigation on QC systems has started on single rare earth ion doped-fluorides capable of a cascade emission such as Pr^{3+}, Tm^{3+}, Er^{3+} and Gd^{3+} [8]. The focus has now been shifted to the combination of two ions, where the energy of a donor ion could be transferred stepwise to two acceptor ions via a down conversion, for example, Gd^{3+}–RE^{3+} [9–11], and RE^{3+}–Yb^{3+} [12–14] .

X-ray, as a high-energy source, can excite RE ions to emit visible light [15–17]. And X-ray phosphor materials have been widely used in the fields of high energy physics, medical imaging, safety inspection, and so on. In order to maintain a short exposure, an X-ray phosphor must be a good absorber of X-rays. It should be a high density compound containing elements with high atomic numbers such as $CaWO_4$, $YTaO_4$, Gd_20_2S, LaOBr, and BaFCl [18]. Furthermore, the phosphor must have good X-ray-to-light conversion efficiency. Nevertheless, the commercially available X-ray phosphor has its own drawback, such as low-luminescent efficiency and hygroscopicity. Hence, developing new high efficiency X-ray phosphors is also a meaningful work. Moreover, QC process appears to be a good way to improve X-ray-to-light conversion efficiency. To the best of our knowledge, there is no previous report about QC excited by X-ray.

$Ba_5Gd_8Zn_4O_{21}$ contains elements with high atomic numbers, Ba and Gd and stable crystal structure may be a good X-ray phosphor. In this paper, host material $Ba_5Gd_8Zn_4O_{21}$ was developed for exploring X-ray phosphor. White light emission, QC, as well as afterglow luminescence of $Ba_5Gd_8Zn_4O_{21}$:Eu^{3+} were studied in details and the mechanism of afterglow luminescence of Eu^{3+} excited by X-ray was investigated.

2. Experimental procedures

The $Ba_5Gd_{8(1-x)}Eu_xZn_4O_{21}$ (x = 0.05%, 0.5%, 1%, 2%, 5%, and 10%) phosphors were synthesized by a high-temperature solid-state reaction method. The starting materials, $BaSO_4$, Gd_2O_3, Eu_2O_3 and ZnO were all analytical reagent (AR) grade. The stoichiometric reactants were mixed and ground thoroughly in an agate mortar. Then,

* Corresponding author. Tel./fax: +86 312 507942.
E-mail address: mihuyym@163.com (Y. Yang).

0925-8388/$ - see front matter © 2013 Elsevier B.V. All rights reserved.
http://dx.doi.org/10.1016/j.jallcom.2013.04.193

the mixture was heated at 1200–1400 °C for 3 h in air atmosphere. After that, the products were cooled down slowly to room temperature. The obtained products were $Ba_5Gd_8Zn_4O_{21}$:Eu^{3+} phosphors.

The structure of the final products were characterized by XRD in a Bruker AXS D8 advanced automatic diffractometer (Bruker Co., German) with Cu $K_{\alpha 1}$ radiation (λ = 1.5406 Å). The emission and excitation spectra were measured using Hitachi F-4600 fluorescence spectrophotometer equipped with a 150 W xenon lamp. The emission chromaticity coordinates of the phosphors were carried out by a UV–VIS-near-IR spectrophotometer (PMS-50). The afterglow images were obtained through a Pentax digital SLR camera. The monitoring and imaging experiments were conducted in a darkroom. All of the measurements were conducted at room temperature.

3. Results and discussion

The XRD patterns of phosphor $Ba_5Gd_8Zn_4O_{21}$:1%Eu^{3+} is shown in Fig. 1 curve (a) shows the standard data (JCPDS51-1686) of pure $Ba_5Gd_8Zn_4O_{21}$ and curve (b) is the XRD patterns of $Ba_5Gd_8Zn_4O_{21}$:-Eu^{3+} in which the Eu^{3+} mole fraction is 1%. All of the observed peaks of the curve (b) herein matched the curve (a), indicating that dopant did not cause any significant changes to the host structure. The crystal structure of $Ba_5Gd_8Zn_4O_{21}$:Eu^{3+} is of a tetragonal phase with 14/m (87) space group. The lattice parameters are a = 1.391087 nm, b = 1.391087 nm, c = 0.576451 nm, and the unit cell volume is 1.1155 nm^3.

The photoluminescence excitation spectra of $Ba_5Gd_{8(1-x)}Eu_xZn_4O_{21}$ (x = 0.05%, 0.5%, 1%, 2%, 5%, and 10%) phosphors monitored at 628 nm are shown in Fig. 2a–f. In Fig. 2c and f, the broad band consists both the O^{2-}–Eu^{3+} and O^{2-}–Gd^{3+} charge transfer band (CTB) and the f–f transitions of Gd^{3+} from $^8S_{7/2}$ to ^6D_J (245 nm), ^6I_J (274 nm), and ^6P_J (313 nm) [19]. In addition, other sharp peaks $^7F_0$–$^5D_4$ (364 nm), $^7F_0$–$^5G_{2,3}$ (384 nm) and $^7F_0$–$^5L_6$ (395 nm) corresponding to the inner 4f-shell excitations of the Eu^{3+} ion are also identified. It's worth mentioning that as the concentration of Eu^{3+} ions was increased, an obvious intensity ratio enhancement of CTB from O^{2-}–Eu^{3+} to the absorption peak at 274 nm from Gd^{3+} was observed in $Ba_5Gd_8Zn_4O_{21}$:Eu^{3+} phosphor as shown in Fig. 2, which indicated that red light emission came mainly from O^{2-}–Eu^{3+} CTB absorption when the concentration of Eu^{3+} ions was higher.

Fig. 3 shows the emission spectra of $Ba_5Gd_8Zn_4O_{21}$:xEu^{3+} (x = 0.05%, 0.5%, 1%, 2%, 5%, and 10%) under 395 nm excitation. The characteristic emissions from $^5D_3$, $^5D_2$, $^5D_1$ and $^5D_0$ excited states to ^7F_J (J = 1, 2, 3, 4) ground states of Eu^{3+} were observed, including $^5D_3$–$^7F_1$ (420 nm), $^5D_3$–$^7F_2$ (430 nm), $^5D_3$–$^7F_3$ (450 nm), $^5D_3$–$^7F_4$ (464 nm), $^5D_2$–$^7F_1$ (473 nm), $^5D_2$–$^7F_2$ (498 nm), $^5D_2$–$^7F_3$ (515 nm), $^5D_1$–$^7F_1$ (540 nm), $^5D_1$–$^7F_2$ (555 nm), $^5D_1$–$^7F_3$ (571 nm), $^5D_0$–$^7F_1$ (597 nm), $^5D_0$–$^7F_2$ (628 nm), $^5D_0$–$^7F_3$ (656 nm) and $^5D_0$–$^7F_4$ (689 nm). The electric dipole transition, $^5D_0$–$^7F_2$ is dominant in the emission spectrum, which indicates that Eu^{3+} ions are located at anti-inversion symmetry in the $Ba_5Gd_8Zn_4O_{21}$ crystals [20,21]. Moreover, the $^5D_3$, $^5D_2$, $^5D_1$ to ^7F_J emission peaks are strong, which can be attributed to the low phonon energy of the host lattice and repressed the multiphonon relaxation.

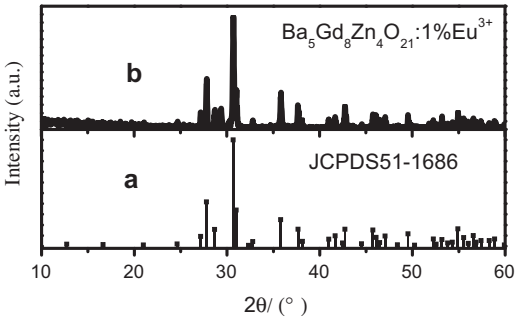

Fig. 1. XRD patterns of $Ba_5Gd_8Zn_4O_{21}$:1%Eu^{3+} phosphor.

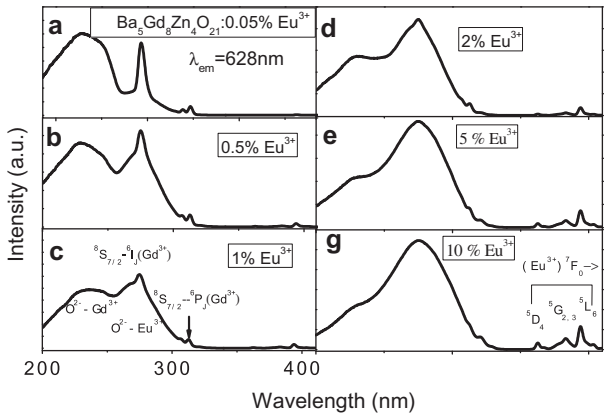

Fig. 2. The excitation spectra of $Ba_5Gd_8Zn_4O_{21}$:xEu^{3+} (x = 0.05–10%) phosphors monitored at 628 nm.

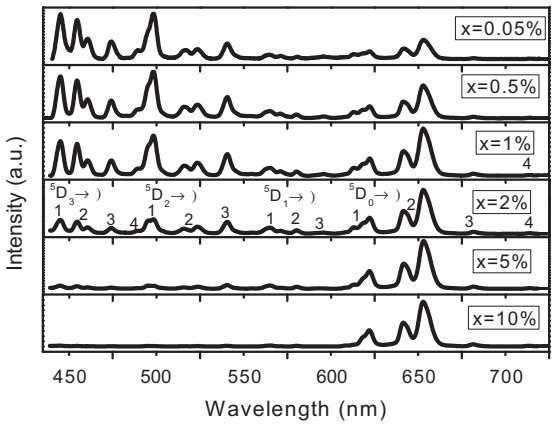

Fig. 3. PL spectra of $Ba_5Gd_8Zn_4O_{21}$:xEu^{3+} (x = 0.05–10%) under 395 nm excitation.

It's worth noting that the luminescence intensity emitting from the higher levels of $^5D_3$, $^5D_2$, and $^5D_1$ decreased relative to that from the low one, $^5D_0$, when the Eu^{3+} concentration increases. It is considered to be the effect of the cross-relaxation from ^5D_J to $^5D_{J-1}$, such as Eu^{3+} ($^5D_1$) + Eu^{3+} ($^7F_0$) → Eu^{3+} ($^5D_0$) + Eu^{3+} ($^7F_3$), for the high concentration of Eu^{3+}, that would shorten the Eu^{3+}–Eu^{3+} distance [22]. As a result, the luminescence color of $Ba_5Gd_8Zn_4O_{21}$:xEu^{3+} can be tuned by changing the doping concentration of Eu^{3+}. Fig. 4 shows the corresponding CIE (Commission Internationale de l'Eclairage 1931 chromaticity) coordinates positions. In this figure, A, B, C, D, E, F points represent the chromaticity coordinates for the Eu^{3+} doped $Ba_5Gd_8Zn_4O_{21}$ phosphors with 0.05, 0.5, 1, 2, 5 and 10 mol%, respectively. It is observed that the (x, y) coordinates of the phosphors vary systematically from (0.256, 0.176) to (0.628, 0.327), with the increase of Eu^{3+} contents from 0.05 to 10 mol%, corresponding to the change of emission color from blue to red. It can be noticed that with increasing Eu^{3+} concentration from 0.5 to 2 mol%, the CIE coordinates change from x = 0.283, y = 0.213 (cold white) to x = 0.420, y = 0.290 (warm white). The white color points are not close to the blackbody locus due to the relative weak green emission [23].

Fig. 5 shows the emission spectra of $Ba_5Gd_8Zn_4O_{21}$:1%Eu^{3+} excited by X-ray, UV-light 274 nm and 395 nm, respectively. Obviously, the red[1] emission upon X-ray and 274 nm excitation is stronger than that of 395 nm, as shown in the inset of Fig. 5. This

[1] For interpretation of color in Fig. 5, the reader is referred to the web version of this article.